Powder Technology 448 (2024) 120274

Contents lists available at ScienceDirect

Powder Technology

journal homepage: www.journals.elsevier.com/powder-technology

Influence of spray parameters on injected droplets and product properties in fluidized bed spray granulation

Maike Orth [a,*], Matthias Börner [b], Swantje Pietsch-Braune [a], Stefan Heinrich [a]

[a] Institute of Solids Process Engineering and Particle Technology, Hamburg University of Technology, Denickestraße 15, Hamburg, 21073, Germany
[b] Hüttlin GmbH, A Syntegon Company, Hohe-Flum-Straße 42, Schopfheim, 79650, Germany

HIGHLIGHTS

- Spray parameters were correlated with droplet and agglomerate properties.
- A three-phase nozzle with additional protection air stream was characterized.
- Investigation of process-related variables in combination with varied nozzle set-up.
- Agglomerate size was primarily influenced by spray rate as well as nozzle and fluidization air streams.

GRAPHICAL ABSTRACT

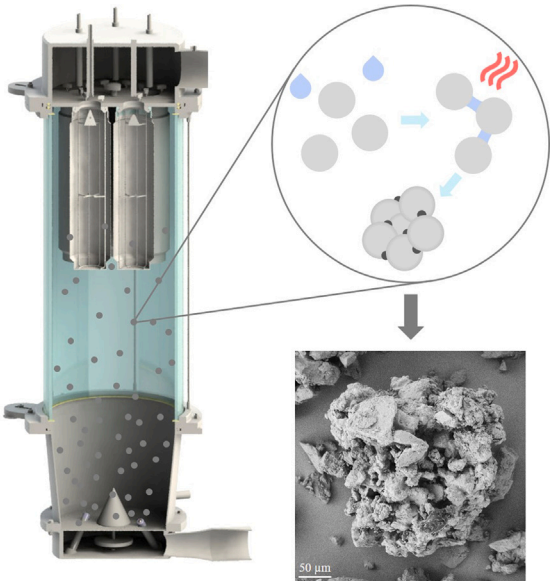

ARTICLE INFO

Keywords:
Fluidized bed
Granulation
Agglomeration
Droplet properties
Spray analysis
Product properties

ABSTRACT

Liquid injection is one of the, if not the most, critical steps in fluidized bed spray granulation as the product quality as well as the overall process stability can be massively influenced by the associated parameters. Therefore, this study aims to correlate spray parameters to the spray pattern and droplets produced from the nozzle and the resulting granule properties. First, the effect of spray variables on spray angle and droplet size and velocity was analyzed, revealing the spray air pressure as crucial parameter. Afterwards, spray agglomeration experiments were conducted according to a statistical experimental plan varying several process-related parameters in addition to the nozzle set-up. The product particle size distribution was shown to be impacted by a complex combination of the investigated variables with the liquid spray rate, spray and protection air pressure, and fluidization air flow as main influences.

* Corresponding author.
E-mail address: maike.orth@tuhh.de (M. Orth).

https://doi.org/10.1016/j.powtec.2024.120274
Received 11 June 2024; Received in revised form 28 August 2024; Accepted 9 September 2024
Available online 1 October 2024

1. Introduction

1.1. Fluidized bed spray granulation

A large proportion of industrial goods, intermediate products as well as consumables is present in solid, more specifically, particulate form [1,2]. Consequently, processes for the production and handling of solids, such as fluidized bed spray granulation, are of great importance for various industries, including pharmaceuticals, chemicals, and food products. In most cases, a dust-free and free-flowing behavior is desired, which enables a simplified handling of the powder. Depending on the application, additional requirements must be met, e.g. a fast and complete reconstitution for instant food powders [3,4]. For pharmaceutical applications, a uniform distribution of critical quality attributes and active ingredient is essential to achieve a high product quality and precise dosage and release of active components.

Granulation often describes particle formulation and size enlargement processes in general with wet granulation referring to growth due to addition of a solid-containing liquid phase. Two different growth mechanisms are distinguished, coating or layering growth and agglomeration [5]. In case of coating, the injected liquid droplets collide with the particle and spread on the surface. Due to evaporation of the liquid, a solid layer is formed around the particle [6]. In agglomeration, the liquid binds primary particles together to form stable clusters. Upon the collision of two or more wet particles, liquid bridges are created and transformed into solid bridges due to subsequent drying. In contrast, size reduction can occur due to abrasion and breakage of solid particles or rupture of liquid bridges if viscous and capillary forces are too small [7]. In this work, a fluidized bed spray agglomeration process is investigated.

The formation of agglomerates and consequently the properties of the final product are dependent on the process parameters during fluidized bed processing. One critical step is the spraying of liquids into the particle bed. One the one hand, droplet characteristics like size and velocity, that influence the interaction between solid particles and liquid droplets, are affected by critical process parameters such as liquid spray rate and spray air pressure. One the other hand, the spray pattern and local particle motion are influenced by spray-related process variables as well as geometry and position of the nozzle. To achieve the desired agglomerate properties, suitable spray parameters, that ensure a stable process and high product quality, need to be chosen.

1.2. Liquid injection into fluidized beds

A nozzle type commonly used for liquid injection in fluidized bed processes are two-fluid nozzles [8]. In this type of nozzle, a liquid stream is atomized by a gas flow due to the shear forces acting on the liquid. The significantly higher gas velocity compared to the velocity of the liquid and the resulting forces cause the liquid to break up into filaments and subsequently into fine droplets. Depending on the gas and liquid velocities, droplets with different sizes and velocities are created. The ratio of gas flow to liquid flow is referred to as gas-to-liquid ratio or air-to-liquid-ratio (ALR) in case of air as atomizing gas [9]. Two-fluid nozzles can be distinguished into nozzles with internal or external mixing. In the former, the liquid is injected into a gas stream, whereas in the latter both phases come into contact at the nozzle outlet [10].

To introduce the liquid droplets into a fluidized bed, one or multiple nozzles can be installed in different positions. Most commonly, the top-spray configuration is applied, in which the nozzle is placed facing downwards above the particle bed. Due to the large surface of the particle bed exposed to the droplets, contact between liquid and particles is promoted. However, the fluctuating bed height and thus varying flight times and distances of the droplets might cause a non-uniform distribution of liquid on the particles as well as an increased risk of spray drying of droplets before a collision with a particle occurs [11–13].

To reduce droplet airborne time and distance, the nozzle can also be installed in bottom-spray configuration with the nozzle positioned in the distributor plate spraying upwards into the particle bed. While the risk of spray drying is consequently reduced, direct wetting of the product occurs. In the worst case, inhomogeneous wetting can lead to local overwetting, lump formation, and collapse of the fluidized bed [11].

Furthermore, a modified bottom-spray approach, the Wurster coater, can be applied to induce a structured particle flow and more uniform liquid distribution. By installing a vertical draft tube centrally over a special distributor plate with a higher orifice diameter in the area beneath the tube, the gas velocity in the central area is enhanced resulting in a circulating particle motion. Hence, a distinct wetting zone and drying zone are created [11,14,15].

1.3. Previous works

Several existing studies are concerned with the influence of material and process parameters on agglomerate growth and properties in fluidized bed spray agglomeration. Mostly, a one-factor-at-a-time approach was used or a limited number of parameters were investigated.

Hemati et al. [16] analyzed how process-related variables, such as nozzle position, atomizing air flow rate, fluidizing air velocity, and liquid spray rate, as well as material properties affect the injected droplets and growth rate of agglomerates in a top-spray fluidized bed. An enhanced growth rate was observed at the lowest distance between nozzle and particle bed, low spray air flows, high spray rates, and decreased fluidization air velocities. Increasing the spray air flow furthermore resulted in a more homogeneous distribution of the binder over the surface of the primary particles due to the higher number and smaller size of the injected droplets.

Similar trends concerning the agglomerate growth rate were observed by Bouffard et al. [17] and Vengateson and Mohan [18] when varying the binder spray rate and fluidization air velocity. However, Bouffard et al. [17] also reported that the agglomeration was not significantly affected by the different droplet sizes produced at varied atomization pressure. Moreover, the binder concentration in the spray liquid was identified as crucial influence on the agglomeration mechanism with an enhanced agglomerate size at high concentrations.

Dadkhah and Tsotsas [19] performed agglomeration experiments with porous as well as non-porous particles in a top-spray fluidized bed, varying the inlet air temperature and binder concentration in the spray solution. In addition to the growth of agglomerates, the internal particle structure was analyzed using X-ray tomography. Again, the binder concentration had a major impact on the agglomeration process, similar to the trend described in [17]. The larger agglomerates produced at high concentrations showed a greater porosity compared to the small agglomerates from experiments with low binder concentrations. When increasing the air temperature, smaller and denser agglomerates were produced.

Lipps and Sakr [20] created a response surface methodology design including binder spray rate and inlet air temperature. A quadratic model was then used to describe the influence of these parameters on several agglomerate properties, such as size, specific surface area, and density, among others. The mean agglomerate size increased with increasing liquid flow rate and decreasing air temperature.

A response surface design was also used by Wang et al. [21] to investigate the influence of binder viscosity and spray rate, fluidization gas velocity, and inlet gas temperature on agglomeration behavior of glass beads in a top-spray fluidized bed. Similarly to the previously mentioned studies, a higher product size and lower sphericity resulted from increasing the spray rate and binder concentration due to the higher binder content in bed and increased viscosity. In contrast, an

increased gas velocity and temperature lead to the formation of smaller agglomerates.

Kemp et al. [22] developed and validated a mechanistic model to describe the impact of four process parameters on moisture accumulation and peak moisture content during fluidized bed spray agglomeration. For this, the inlet air temperature, flow rate and humidity were summed up in the heat input and evaluated together with the liquid spray rate. High ratios of heat input to spray rate caused less moisture accumulation and a lower maximum moisture content during agglomeration, which lead to a smaller product size due to the weaker binding between particles. In contrast, high moisture levels favored the formation of large agglomerates by providing a larger amount of liquid binder for bridge formation.

A continuous agglomeration process was investigated by Strenzke et al. [23]. In addition to process variables specifically connected to continuous operation, the binder spray rate, binder concentration, spray air flow, fluidization air flow, and inlet air temperature were varied. Similar trends as in the other studies presented were observed: A high spray rate and binder concentration as well as low temperatures and air flows for atomization and fluidization favored growth and resulted in the production of larger agglomerates. Agglomerate structure, as characterized by the porosity and sphericity, was only marginally influenced.

Du et al. [24] observed similar effects of the inlet gas temperature and binder concentration in a continuous agglomeration process in top-spray configuration: A reduced temperature lead to faster growth of agglomerates and a wider particle size distribution due to more moderate drying conditions. Larger particles were produced when increasing the binder concentration. Above a critical concentration however, the high viscosity caused particle over-wetting near the nozzles, which eventually lead to defluidization and collapse of the fluidized bed.

Further works, e.g. [25,26], discuss the influence of material characteristics of the primary particles as well as the binder liquid on agglomerate growth and product properties.

However, a comprehensive study including evaluation of the influence of numerous parameters as well as their interactions is still needed. Therefore, this work aims to investigate the combined effect of process parameters that affect the spray as well as variations of the nozzle set-up on agglomerate formation in order to qualitatively and quantitatively explain the multidimensional correlations between spray parameters and product properties.

2. Materials and methods

2.1. Materials

As primary particles, the monohydrate lactose *Lactochem*® Fine Powder (DFE Pharma, Germany) was used. Lactose is commonly used as an excipient in pharmaceutical industry, being present in 60 – 70 % of registered oral solid dosage formulations such as tablets [27]. With a mean diameter of 50 μm, the milled lactose used in this study is well suitable for structurization in a fluidized bed and a potential subsequent compaction step [28].

As binder the water-soluble polymer polyvinylpyrrolidone (PVP) with a K-value of 30 was used, which is a common additive in pharmaceutical formulations. During agglomeration experiments, an aqueous solution containing 25 wt% PVP was injected. The solution showed Newtonian flow behavior and the viscosity was measured to be 72.1 ± 5.3 mPas at 20 °C. The combination of lactose and PVP is used as a model system to form representative structures for solid pharmaceutical products.

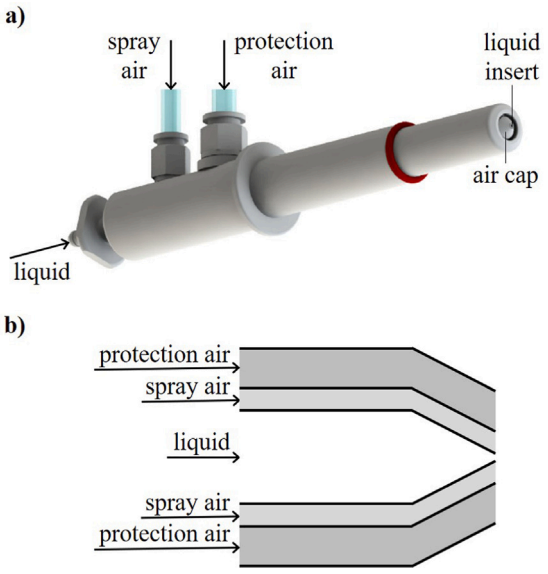

Fig. 1. Three-fluid nozzle used in agglomeration experiments: (a) CAD model, (b) scheme of nozzle outlet.

2.2. Nozzle characterization

For the injection of the binder liquid into the fluidized bed, two three-fluid nozzles as shown in Fig. 1 (Syntegon Technology, Germany) were used. In addition to the spray liquid and the atomization gas, a second gas stream through the nozzle, the protection gas, prevents particles from sticking to the nozzle tip. Pressurized air is used as spray and protection gas. Both, the orifice diameter for the liquid as well as the gap width for the spray air can be varied by changing the liquid insert or air cap, respectively.

To characterize the spray pattern and the droplets and consecutively their influence on agglomerate formation, the nozzle was investigated with regard to spray cone angle as well as droplet size and velocity. The spray angle measurement was conducted according to the method described in [29]. Therefore, the spray cone at different nozzle settings was recorded using a high-speed camera (*NX-S2*, Imaging Solutions GmbH, Germany). Afterwards, the images were post-processed and analyzed using the software *MATLAB* (the MathWorks, Inc., USA). As part of this, the grayscale images were converted to binary images according to a threshold based on the peak in the histogram over all gray levels in the images. In these images, the outlines of the white spray cone on the black background were detected and approximated by linear functions, from which the spray cone angle was calculated. An exemplary binary image is shown in Fig. 2. Water was used as spray liquid and compressed air as atomizing gas. Images were recorded and evaluated at spray rates ranging from 20 to 60 g/min, spray air pressures from 0.5 to 3.0 bar, and protection air pressures from 0.1 to 0.3 bar using three different air caps with the orifice diameters 2.3, 3.0, and 3.8 mm.

To determine the droplet size and velocity, the *SpraySpy*® *LabLine* system (AOM-Systems GmbH, Germany) was used. The measurement principle is based on light scattering of a moving droplet that is illuminated by a beam of light. The scattered light is then separated into its individual scattering orders and registered by photodetectors. Using the characteristics of the scattering order, the mean droplet size and mean velocity can be obtained [30]. For all runs, a solution of 25 wt% PVP and 75 wt% water was sprayed and atomized by compressed air. Droplets were analyzed in the radial center of the spray cone at a distance of 15 cm from the tip of the nozzle at a constant protection air pressure of 0.2 bar. Three different air caps with orifice sizes 2.3, 3.0, and 3.8 mm were tested at different spray rates (6–472 g/min) and spray air pressures (0.5–3.0 bar).

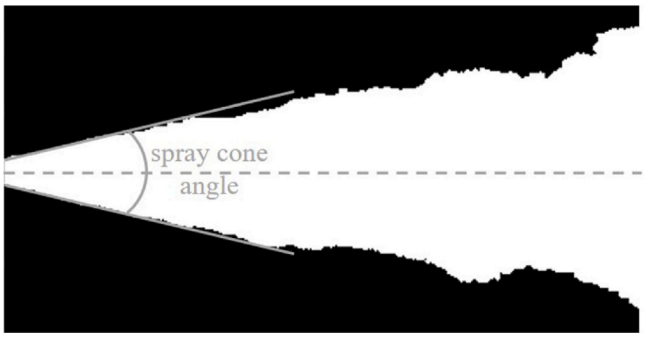

Fig. 2. Binary image of spray cone of three-fluid nozzle to evaluate the spray cone angle.

Table 1
Varied process parameters and nozzle set-ups.

Parameters	Values	Unit
Liquid spray rate	40 – 120	g/min
Spray air pressure	0.5 – 3.0	bar
Protection air pressure	0.1 – 0.3	bar
Fluidization air volume flow	130 – 200	m^3/h
Nozzle inclination angle	40, 50, 60	°
Air cap orifice diameter	2.3, 3.0, 3.8	mm

2.3. Agglomeration experiments

Fluidized bed agglomeration experiments were performed in a laboratory scale prototype developed at Syntegon Technology (Germany), which is shown in Fig. 3. The fluidization gas enters the apparatus through a tangential air inlet and a flat windbox, which creates a spiral air flow pattern. Above the windbox, the *Diskjet* distributor, a stainless steel plate with a diameter of 300 mm and a radial pattern of narrow slits of 0.2 mm width with a 45° inclined guidance, supports the oblique gas flow into the particle bed. In the center of the distributor, a stainless steel cone of 90 mm height and 80 mm diameter is placed to ameliorate the particle movement near the bottom. Two three-fluid nozzles (see Section 2.2) are placed in bottom spray position with an inclination of 40°, 50°, or 60° each at 80 mm distance from the center of the *Diskjet*. Fig. 4 depicts the different inclination angles in which the two nozzles can be installed.

All experiments were carried out batch-wise with an initial bed mass of 3 kg lactose and inlet temperature of the fluidization air of 80 °C. 600 g of binder solution were sprayed each run. In order to evaluate the influence of spray related parameters on the agglomerates produced in the fluidized bed, a statistical experimental plan was created including six variables, related to either the process or apparatus design. The design of experiment software *Design-Expert* (Stat-Ease, Inc., USA) was used to create a D-optimal design, which offers the possibility to combine continuous and discrete numeric factors as well as to set a unique number of levels for each discrete factor [31]. To generate the design, the covariance of the least-square estimates of the parameters is minimized for a beforehand defined model by an iterative algorithm. An experimental plan consisting of 31 experiments, with which linear, two-factor interaction, and quadratic effects can be considered, was created. Compared to a two-level full factorial plan with six parameters, which would result in 64 runs, the experimental effort is significantly reduced when using a D-optimal design. Varied parameters as well as their limits or discrete values are listed in Table 1. The whole experimental plan can be found in the appendix.

2.4. Particle characterization

To characterize the produced agglomerates, the particle size distribution and particle structure were analyzed. For the particle size distribution measurement, the *Camsizer XT* (Retsch GmbH, Germany) was used, equipped with the air pressure dispersion module (*X-Jet*). After falling from a vibrated chute, the particles are entrained by pressurized air to separate particles sticking together due to cohesive or electrostatic forces. The particle size is determined based on an optical measurement from images recorded by two cameras.

In addition to evaluating the mean particle size, the whole particle size distribution was analyzed with regard to the overall shape. Therefore, the standard deviation of the distribution was calculated. An advantage of the standard deviation in comparison to other characteristic values such as the SPAN value is that in addition to the width also the shape of the distribution is considered.

To evaluate the agglomerate structure, selected samples were analyzed with the scanning electron microscope *Supra VP55* (Zeiss, Germany).

Table 2
Reynolds number of spray air for investigated pressures and air caps.

		Spray air pressure [bar]		
		0.5	1.75	3.0
Air cap orifice diameter [mm]	2.3	$1.4 \cdot 10^7$	$2.5 \cdot 10^7$	$2.5 \cdot 10^7$
	3.0	$1.8 \cdot 10^7$	$4.1 \cdot 10^7$	$4.1 \cdot 10^7$
	3.8	$1.7 \cdot 10^7$	$4.3 \cdot 10^7$	$5.9 \cdot 10^7$

3. Results and discussion

3.1. Spray pattern

Depending on the spray parameters applied to the nozzle, various spray patterns and droplets with different sizes and velocities are created. These characteristics have a major impact on the interaction between liquid and particles in the fluidized bed and thus on the resulting agglomerate properties. Fig. 5 shows the spray cone angle for varied ALRs, protection air pressures, and air cap orifices.

The different ALRs result from changes in liquid spray rate and spray air pressure. For all protection air pressures and all air caps, a decreasing spray angle was observed for an increasing ALR. A higher ALR is either caused by a lowered liquid spray rate and therefore lower liquid velocity or by an increase in spray air pressure that leads to higher air velocity and inertia forces. To evaluate the air flow regime, the Reynolds number at the three investigated pressures was calculated from the air velocity, which in turn was determined from the measured volume flow through the nozzle and the cross-sectional area between the liquid insert and the air cap. Even though, for all spray air pressures investigated, the air flow is in the turbulent regime, the higher Reynolds numbers at increased air pressures indicate an enhanced turbulence (see Table 2). Thus, with rising ALR, a higher relative velocity between gas and liquid phase is achieved, which increases the frictional forces on the liquid surface as well as the shear forces within the stream. In addition, high velocity air can easily penetrate a low velocity liquid jet, whereas at higher liquid velocities, the liquid stream cannot be penetrated to the same degree [8]. Consequently, at high ALRs, the spray cone is shaped into a narrow form with a low spray angle, while a low ALR leads to a wider radial distribution of the spray at a given distance from the nozzle tip. In case of a nozzle with external mixing, as the one used in this study, the effect of a narrowing spray cone with increasing ALR is further supported by the backflow of air and droplets [10,32]. Similar trends regarding the influence of the ALR on the spray angle were described by Lefebvre [33]. Liu et al. [32] also observed a contraction of the spray cone at higher spray pressure.

As shown in Fig. 5a, the protection air stream has an additional shaping effect on the spray cone with an increase in pressure inducing a decreasing cone angle. This effect is especially pronounced at low ALRs. The highest angle of $33.86 \pm 0.76°$ is achieved at the lowest ALR of 0.37 and lowest protection air pressure of 0.1 bar. In contrast, at an ALR of

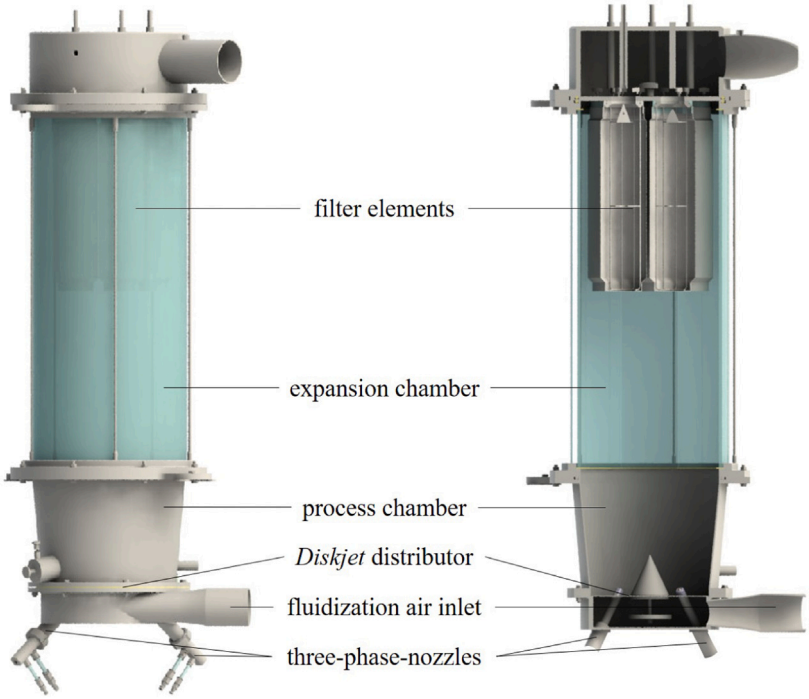

Fig. 3. Fluidized bed set-up for agglomeration experiments.

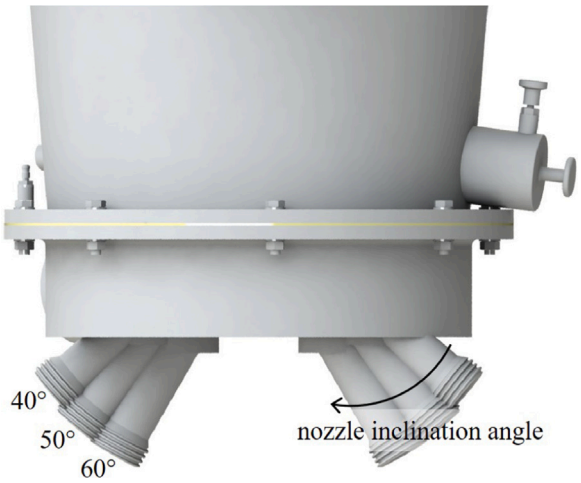

Fig. 4. Different nozzle inclination angles for the prototype fluidized bed.

4.70 and protection air pressure of 0.3 bar, the narrowest spray pattern with an angle of 19.21 ± 0.72° was created due to the additional energy introduced into the system by both, the spray air and the protection air. Fig. 6 shows exemplary images of spray cones recorded at different parameter settings.

At high ALR as well as at high protection air pressure, the effect of spray variables on the spray cone angle is less pronounced compared to the measurement at lower gas velocities. Taking into account the relation between the air mass flows and pressures depicted in Fig. 7, a change in flow behavior can be observed when reaching a certain critical pressure. This effect occurs for both air streams, spray air (Fig. 7a) and protection air (Fig. 7b). At low pressures, the correlation to the mass flow is non-linear and contains at least quadratic dependencies. When increasing the pressure up to a critical point, the air velocity reaches sonic speed, which changes the air flow. For example, this point is reached at approximately 1 bar when using an air cap with 2.3 mm orifice. From this point on, the air mass flow increases linearly with pressure due to the constant velocity at the nozzle outlet. As consequence of this relation between air flow and pressure, the impact on the spray cone angle declines with increasing air velocity and thus ALR, as can be seen from the decreasing slope in Fig. 5.

The influence of the air cap on the spray angle is depicted in Fig. 5b. For an orifice size of 3.0 mm and 3.8 mm, a similar trend can be observed. The spray angle falls from just below 40° at 0.37 ALR to 24.64 ± 1.67° for 3.0 mm and 27.23 ± 3.09° at 4.70 ALR, respectively. A falling trend of the angle over the ALR can also be seen for the 2.3 mm air cap orifice. However, with a decrease of only 5.65° over the same ALR range the trend is less pronounced than for the larger orifices. Furthermore, the spray angles measured for the smallest air cap are significantly lower compared to larger gap sizes. Due to the smaller cross-sectional area available for the air when choosing a smaller air cap, a higher gas velocity is reached at the same air mass flow and thus ALR. The therefore higher relative velocity between gas and liquid results in larger forces acting on the liquid jet, consequently creating a narrower spray cone. As the pressure, at which sonic speed is reached, is lower the smaller the orifice, the degree to which the spray angle is influenced by the ALR varies with the air cap.

However, using X-ray imaging Newton et al. [34] found that spray angles of single slot and multiport nozzles were smaller in the fluidized bed than in open air. In addition, Ariyapadi et al. [35] showed that for a straight-tube nozzle, the expansion of the spray cone is dependent on the density of the fluidized bed. These observations suggest that a similar effect could occur with the three-fluid nozzles used in this study, which needs to be considered when referring to the spray cone created during fluidized bed experiments.

3.2. Droplet properties

Not only the spray pattern, but also the droplets produced from the three-phase nozzle are affected by the interactions of liquid and gaseous phase described in Section 3.1. Fig. 8a and 8b show the mean droplet diameter, which corresponds to the median value of the droplet size distribution, and velocity in dependence of the ALR and spray air pressure, respectively. Generally, both representations show a similar

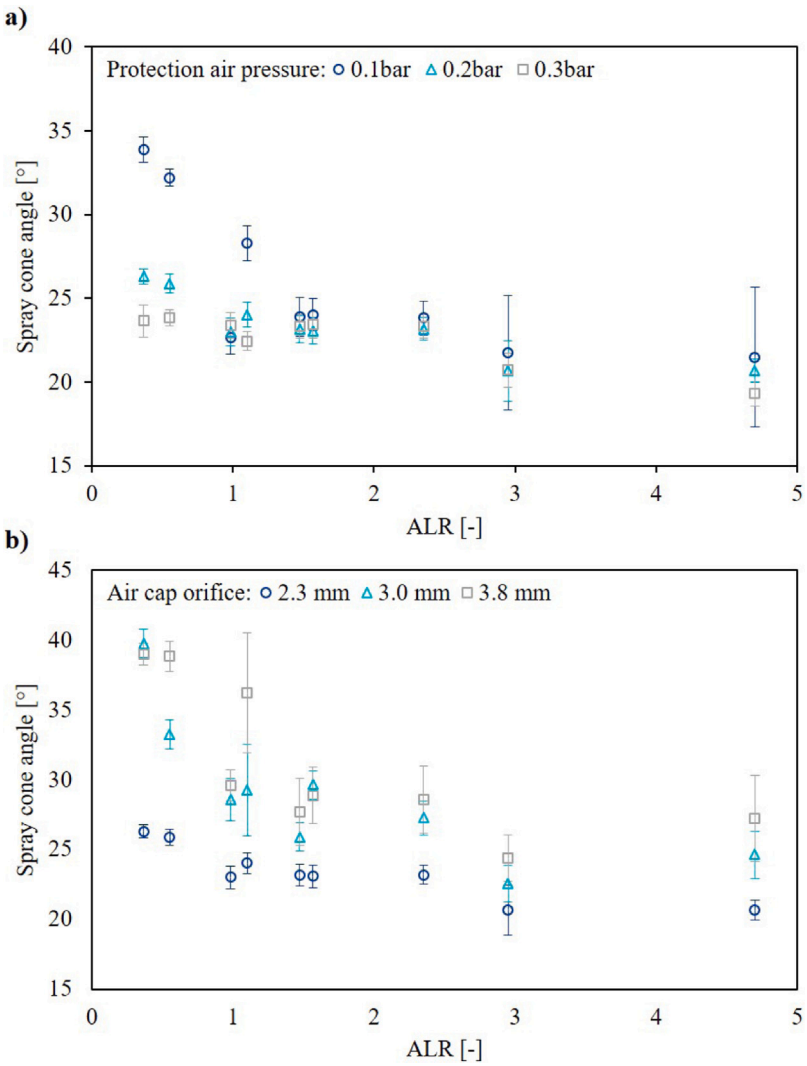

Fig. 5. Spray cone angle at varied ratio of spray air to liquid (ALR): (a) different protection air pressures, air cap orifice: 2.3 mm, (b) different air cap orifices, protection air pressure: 0.2 bar.

trend, a decreasing droplet size and increasing velocity with rising ALR and spray air pressure. These trends appear to be more clear in dependence of the pressure as seen in Fig. 8b, indicating that the pressure is the strongest influence on droplet properties among the investigated parameters. However, it has to be noted that the variation of the liquid spray rate is not marked in this depiction.

As explained in Section 3.1, an increase in spray air pressure and thus velocity leads to higher dynamic pressure forces acting on the liquid, which results in an enhanced shear stress and more effective droplet comminution [9]. Moreover, the backflow of droplets and gas associated with the increased relative velocity between both phases further supports the creation of fine droplets [10,32]. In contrast, a higher liquid flow rate and therefore lower ALR results in the creation of larger droplets as the liquid jet cannot be as easily penetrated by the gas [8]. The observed trends concerning the mean droplet size are in agreement with the results of Rizk and Lefebvre [36] and Vesey et al. [37]. The importance of the influence of the ALR and relative velocity between air and liquid on droplet formation is also highlighted by several correlations to calculate the droplet size, e.g. by Mulhem et al. [9] or Walzel [38].

Another factor that affects droplet size is the viscosity of the liquid. As reported by Mulhem and Schulte [9] and Vesey et al. [37], an increased viscosity negatively impacts the break up of the liquid and therefore the production of larger droplets. Since a PVP solution was used in this study, the increased viscosity in comparison to water is also assumed to influence the droplet size accordingly.

Droplet velocity was measured in the center of the spray cone, where the highest velocities occur [37]. Again, the spray air pressure was identified as dominant influence, that seemingly overshadows the influence of the liquid velocity due to conveying the liquid itself. When increasing the spray air pressure and ALR, higher droplet velocities are obtained due to the high velocity gas stream dragging the droplets along. In addition, the finer droplets created at higher ALR can be easier accelerated by the gas stream compared to larger droplets, increasing their velocity even further.

The air cap orifice size did not show as clear an influence on the droplet properties as it did on the spray cone angle. Still, a trend of increase in size and decrease in velocity with increasing orifice size can be observed. The highest mean droplet diameter of 32.6 μm and lowest velocity of 16.4 m/s were reached at the lowest investigated ALR, when using the largest air cap with an orifice size of 3.8 mm.

3.3. Mean agglomerate size

31 agglomeration experiments were performed in the prototype fluidized bed set-up according to the statistical plan generated using the D-optimal design algorithm. As described in Section 1.1, the creation

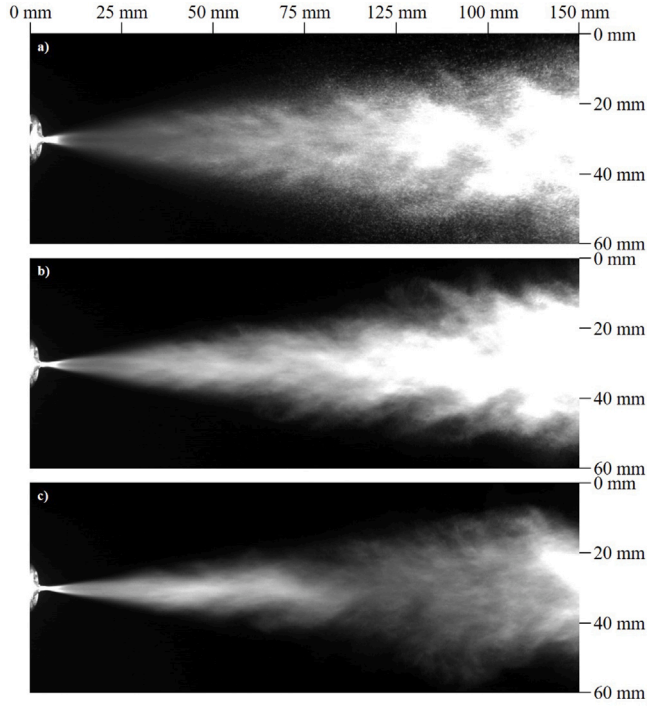

Fig. 6. Spray cones recorded at varied parameters with 2.3 mm air cap orifice: (a) protection air pressure = 0.1 bar, ALR = 0.37, angle = 33.86 ± 0.76°, (b) protection air pressure = 0.2 bar, ALR = 1.47, angle = 23.17 ± 0.80°, (c) protection air pressure = 0.3 bar, ALR = 4.70, angle = 19.31 ± 0.72°.

of agglomerates and their properties are mainly dependent on the formation, potential rupture, and solidification of liquid bridges between primary particles. These phenomena are influenced by the droplet size, droplet and particle motion, and available liquid in the particle bed among others, which are in turn affected by spray parameters. Ennis et al. [39] formulated a viscous Stokes number St_v and a critical Stokes number St_v^* to obtain a criterion for successful agglomeration of two colliding particles:

$$St_v = \frac{2}{3}\frac{m_p \cdot v_0}{\pi \cdot \eta \cdot r^2}, \tag{1}$$

$$St_v^* = \left(1 + \frac{1}{e}\right) \cdot \ln\left(\frac{h_0}{h_a}\right) \tag{2}$$

with the particle mass m_p, particle velocity before collision v_0, liquid layer viscosity η, particle radius r, coefficient of reconstitution e, liquid layer height h_0, and roughness h_a. Successful coalescence is reached if the viscous dissipation is higher than the kinetic energy $\left(St_v \leq St_v^*\right)$. However, it should be noted that the model by Ennis et al. [39] is based on the assumption of non-deformable, spherical particles surrounded by a thin viscous binder layer. Furthermore, capillary forces are neglected as viscous forces are dominant for viscous binders under dynamic conditions. The ratio of viscous to capillary forces is described by the dimensionless capillary number [40]:

$$Ca = \frac{6\eta \cdot (r \cdot g)^{\frac{1}{2}}}{\gamma} \tag{3}$$

with the viscosity η, particle radius r, acceleration due to gravity g, and surface tension γ.

To obtain a model to correlate the investigated parameters in Table 1 to the agglomerate size, an ANOVA with a significance level of 0.05 was used. Following this criteria, 13 significant terms, as indicated by a p-value smaller than 0.05, where included in a quadratic model. Furthermore, the air cap orifice and nozzle inclination angle were added in order to maintain hierarchy. Finally, the following model with $R^2 = 0.96$ was obtained:

$$\begin{aligned} d_{50,3} = {} & 199.0 + 43.5\ \dot{m}_l^2 - 54.8\ p_{pa}^2 + 63.9\ \dot{m}_l - 58.6\ p_{spa} \\ & - 24.7\ p_{pa} - 31.1\ \dot{V}_{fa} - 2.3\ d_{spa} - 6.1\ \alpha_n - 18.4\ \dot{m}_l p_{pa} \\ & - 17.1\ \dot{m}_l \dot{V}_{fa} - 17.0\ \dot{m}_l \alpha_n + 13.0\ p_{spa} p_{pa} - 19.3\ p_{spa} d_{spa} \\ & + 17.1\ d_{spa} \alpha_n \end{aligned} \tag{4}$$

with the mean particle diameter $d_{50,3}$, liquid spray rate $\dot{m}_l$, spray air pressure p_{spa}, protection air pressure p_{pa}, fluidization air volume flow $\dot{V}_{fa}$, diameter of the spray air cap orifice d_{spa}, and nozzle inclination angle α_n. In Eq. (4), the high level of each factor is coded as 1 and low levels are coded as −1 with the units being scaled accordingly. By coding the equation like this, relative impacts of the factors can be identified by comparing the coefficients, which provides a common basis to discuss the effects on agglomerate size. For clarity, all coefficients were rounded to the first decimal place.

The spray rate, spray air and protection air pressure, and fluidization air flow were identified as significant main effects in addition to several interactions. Fig. 9 shows the influence of the main effects on the mean particle diameter in form of contour plots.

With increasing spray rate of the binder solution, larger agglomerates were produced. This observation is confirmed by the scanning electron microscope images in Fig. 10b and 10c, which show agglomerates from experiments with different spray rates. The liquid spray rate affects the availability of binder for the solid particles and bed temperature as well as the droplet size and spray pattern. At higher spray rates, more liquid is injected into to fluidized bed per time interval, which causes a large drop in bed temperature. Consequently, evaporation of binder containing droplets happens comparatively slow. As stated by Kemp et al. [22], the higher moisture accumulation caused by higher spray rates enhances liquid bridge formation and thus supports agglomerate growth. Considering the sticking criterion based on the Stokes number, high availability of liquid increases the liquid layer height and therefore the critical Stokes number, which promotes agglomerate growth [7]. Furthermore, larger droplets and a wider spray cone are created from the three-fluid nozzles at increased spray rate, as explained in sections 3.1 and 3.2. All of these effects contribute to a higher amount of wetted particles and therefore a higher probability of wet particle collisions, which are a crucial step in agglomerate formation. The larger droplet diameter and higher number of injected droplets increase the number of wetted particles as well as the surface area that is wetted during a particle–droplet collision. Hence, more liquid bridges are formed and the liquid available for an individual bridge might be higher, which results in an increased viscous damping force and thus a less likely rupture. Bunke et al. [41] investigated binary wet particle collisions and showed that a higher liquid film on the particle surface resulted in a higher energy dissipation upon collision and consequently an enhanced deceleration. Grohn et al. [42] measured a higher critical bridge length and longer time duration until rupture of a liquid bridge between two particles with increasing bridge volume. As a result of these more stable liquid bridges being formed at higher bridge volumes, the agglomeration tendency is enhanced at increased spray rates.

Due to the higher chance of wet collision in addition to a higher chance of a wet collision being successful in terms of forming a permanent connection between the particles involved, increasing the liquid spray rate results in a larger mean agglomerate diameter. In contrast, at lower spray rates, the opposite effects occur and the lower amount of wet collisions leads to the formation of smaller agglomerates.

As depicted in Fig. 9a, the mean agglomerate size decreases with increasing spray air pressure. The difference in size is also apparent for the exemplary agglomerates shown in Fig. 10b and 10d, where the particle from the experiment with elevated spray air pressure is significantly smaller than the agglomerate produced at low pressure. As explained in the previous section, the spray air pressure is one

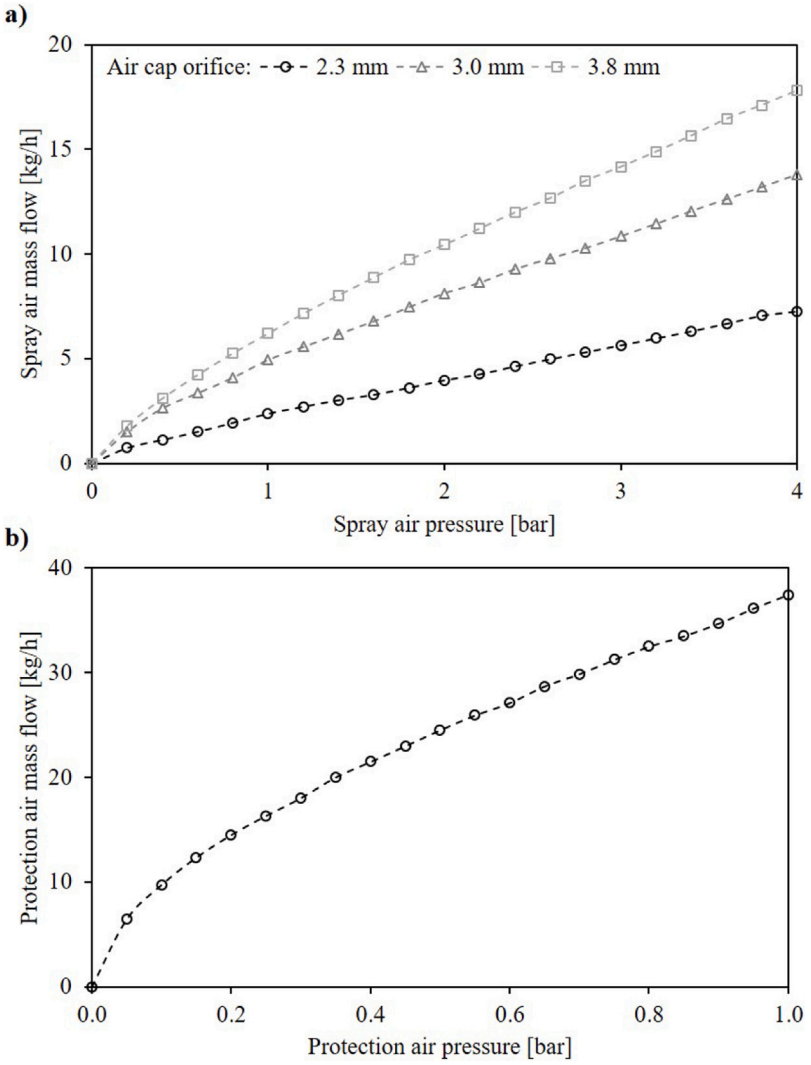

Fig. 7. Spray air mass flow at varied pressure for different air cap orifices.

of the main factors that determine droplet size and velocity, with higher pressures resulting in smaller droplet diameters and enhanced velocities. These small droplets are at a higher risk of being spray dried by the heated fluidizing air and subsequently not available for liquid bridge formation, before colliding with a particle. Furthermore, droplets might be elutriated due to their high velocity in addition to the locally increased bed porosity near the nozzles caused by the high spray air flow. When colliding with a particle, the high velocity enables a better spreading of the droplets [43]. As consequence, the liquid film on the particle surface is lower, which reduces the viscous damping force and thus the agglomeration tendency in case of a wet particle collision. Moreover, the narrower spray cone angle created at high spray air pressures decreases the size of the wetting zone, which in turn lowers the amount of collision of wetted particles in the first place. Although most particles are wetted near the tip of the nozzles, further particles are entrained into the jet and liquid droplets are deposited further away from the nozzles, which emphasized the importance of the spray angle for wetting and agglomerate growth [35]. Another effect to be considered is the possible breakage of agglomerates due to the high shear forces of the spray air acting on the particles. When low spray air pressures are applied on the other hand, the bigger and less accelerated droplets allow the formation of larger agglomerates.

Similar trends as for the spray air pressure can be observed for the influence of the protection air pressure, as shown in Fig. 9b, where an increase in pressure results in a decreasing mean particle size. The effect on spray pattern and droplet properties and subsequently the agglomerate properties are similar to those discussed for the spray air pressure, although less pronounced, as observed in sections 3.1 and 3.2. However, the main purpose of the protection air pressure is not atomization of the liquid, but to protect the nozzle from particles to prevent clogging. Thus, the protection air affects the particle motion in front of the nozzle tip, which in turn determines, where the droplets come into contact with the particles. At increased protection air pressure, particle–droplet collisions occur mostly after a longer flying time of the droplets, after a certain amount of water is already evaporated. With the lower amount of liquid available, agglomeration is less likely, which results in a smaller mean diameter of the product. In contrast, low pressures allow an early contact between droplets and particles near the top of the nozzle before a significant amount of the liquid is evaporated. Therefore, successful wet collisions leading to permanent connections between particles are promoted. For all settings, the nozzle was successfully protected by the additional air stream and no clogging was observed. Hence, the protection air pressure can be used as additional factor to tailor agglomerate properties without compromising nozzle protection.

The last main effect on the mean particle size is the fluidization air volume flow. In Eq. (4) as well as in the contour plot in Fig. 9 a decreasing particle size can be observed with increasing air flow. The fluidization air is the crucial factor for the particle motion in the fluidized bed. When the particles are accelerated by an increased

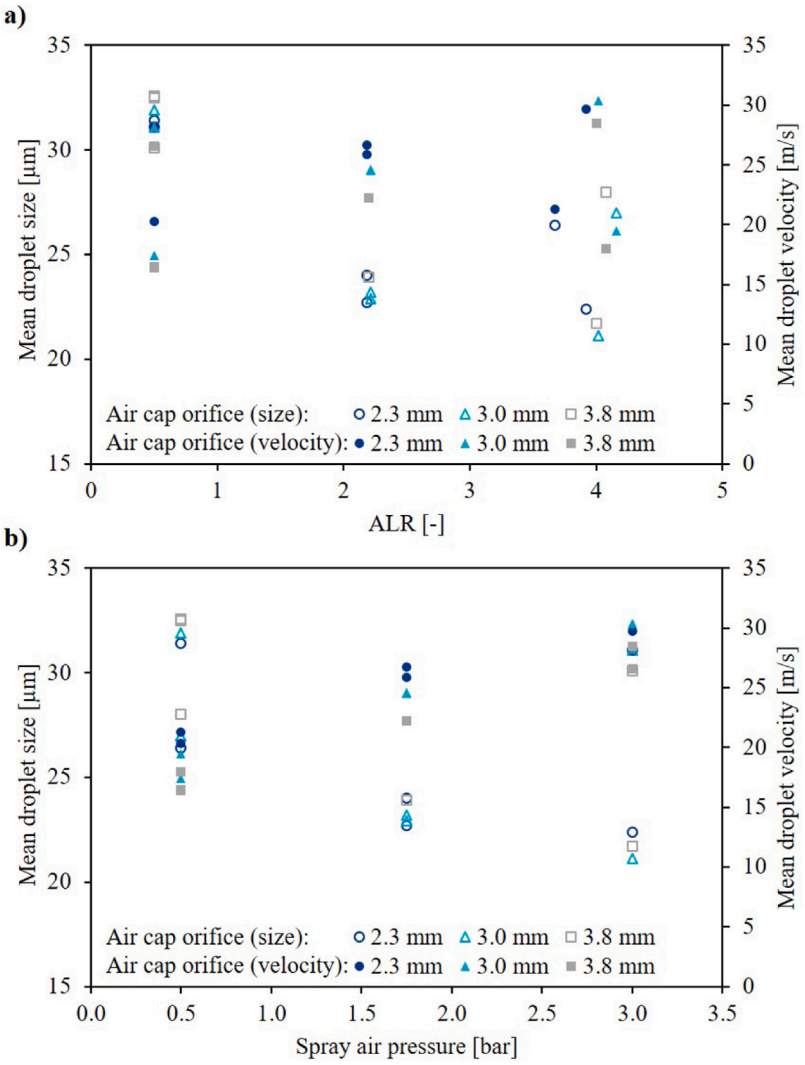

Fig. 8. Mean droplet size and mean droplet velocity at different air cap orifices: (a) varied ratio of spray air to liquid, (b) varied spray air pressure.

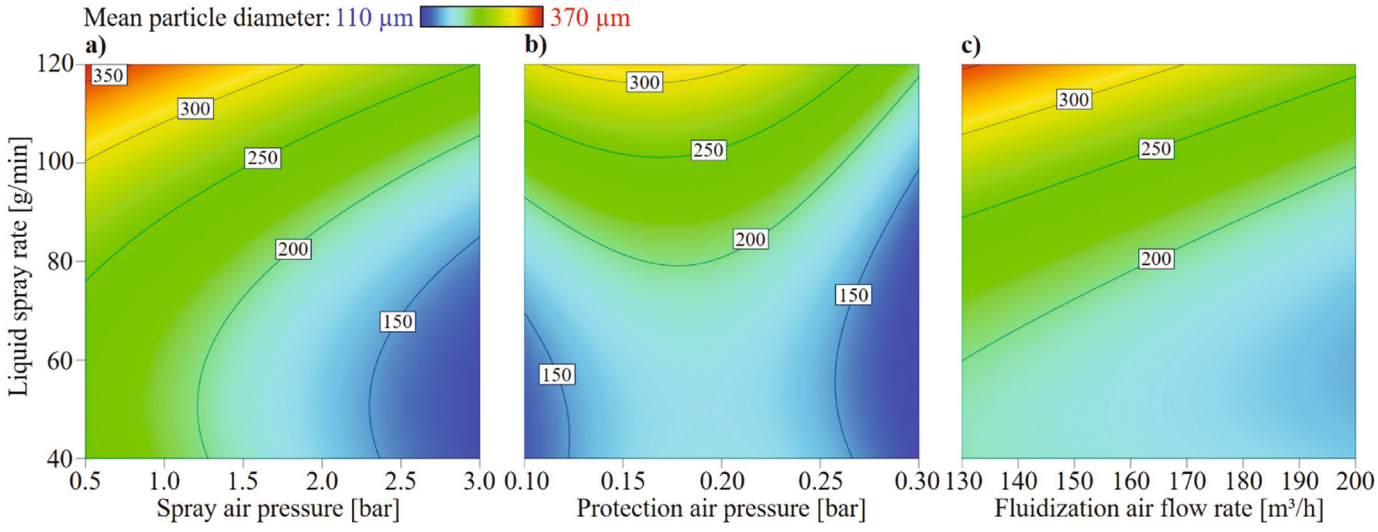

Fig. 9. Mean particle diameter according to quadratic model at varied spray rate and (a) spray air pressure, (b) protection air pressure, and (c) fluidization air flow rate.

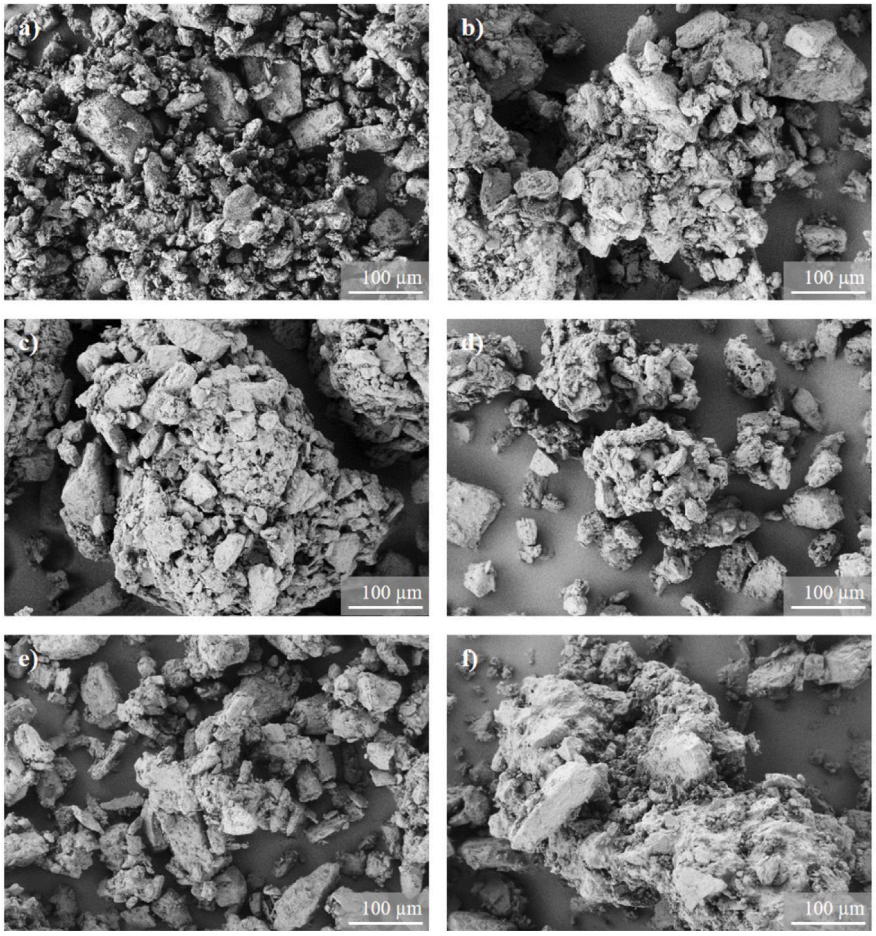

Fig. 10. Scanning electron microscope images of primary particles and agglomerates produced at different spray parameter settings: (a) *Lactochem*®Fine Powder, (b) $\dot{m}_l$ = 40 g/min, p_{spa} = 0.5 bar, p_{pa} = 0.1 bar, $\dot{V}_{fa}$ = 130 m³/h, (c) $\dot{m}_l$ = 120 g/min, (d) p_{spa} = 3.0 bar, (e) p_{pa} = 0.3 bar, (f) $\dot{V}_{fa}$ = 200 m³/h.

volume flow, the bed expands higher, which increases the bed porosity. Due to the additional and larger voids in the bed, that are then created, the flight time and distance of the droplets before colliding with a particle increases. Consequently, the risk of spray drying and droplet elutriation is higher, which lowers the agglomeration tendency. Another factor contributing to the lower product size is the decreased heat input at higher flow rates that reduces moisture accumulation and amplifies the fast drying of droplets and less pronounced bond formation between particles. Moreover, the higher collision velocity caused by an increase of the fluidization air flow enhances the viscous Stokes number, which reduces the probability of a particle–particle collision resulting in coalescence. Collisions between agglomerates with a higher velocity due to an increased air flow or between particles and the apparatus walls are also more likely to result in breakage or attrition, which further reduces particle size. At low fluidization air flows on the other hand, most particles are moving within the lower part of the process chamber, which favors particle–droplet collisions and thus the formation of larger agglomerates.

In addition to the quadratic and linear main effects, complex interactions between certain parameters further influence the mean agglomerate size. For example, the two air streams applied at the nozzles interact with each other. Another significant interaction is the combined effect of spray air pressure and air cap orifice due to the different air flows passing through differently sized orifices to reach the same pressure.

3.4. Standard deviation of particle size distribution

Besides the mean agglomerate size, the width of the particle size distribution needs to be considered to evaluate product quality. Usually, a narrow distribution of product properties is desired to ensure a constant quality. Using the same procedure and statistical criteria as in Section 3.3, a quadratic model with $R^2 = 0.99$ was obtained to correlate the standard deviation of the agglomerate size distribution to various spray parameters:

$$\begin{aligned}\sigma_d = {} & 121.6 + 34.4\ \dot{m}_l^2 - 30.6\ p_{spa}^2 - 45.5\ p_{pa}^2 + 21.3\ d_{spa}^2 + 34.8\ \dot{m}_l \\ & - 33.2\ p_{spa} - 12.2\ p_{pa} - 12.3\ \dot{V}_{fa} - 4.1\ d_{spa} - 0.6\ \alpha_n - 9.6\ \dot{m}_l p_{pa} \\ & - 14.8\ \dot{m}_l \alpha_n + 8.5\ p_{spa} p_{pa} - 15.8\ p_{spa} d_{spa} + 4.5\ p_{pr} \alpha_n \\ & - 8.3\ \dot{V}_{fa} d_{spa} + 13.1 d_{spa} \alpha_n \end{aligned} \quad (5)$$

with the standard deviation of the particle size distribution σ_d, liquid spray rate $\dot{m}_l$, spray air pressure p_{spa}, protection air pressure p_{pa}, fluidization air volume flow $\dot{V}_{fa}$, diameter of the spray air cap orifice d_{spa}, and nozzle inclination angle α_n. The spray rate, fluidization air flow, and air cap orifice size, as well as both pressures were identified as significant main influences. Their influence on the standard deviation is depicted in Fig. 11. Combined with the relevant interactions and the nozzle inclination angle, which was added for model hierarchy, the model contains a total of 18 coefficients.

As explained in the previous section, the additional liquid in the fluidized bed at high spray rates favors the formation and stability of liquid bridges with more wet particles in the system. Consequently, more agglomeration events occur, in which primary particles or already

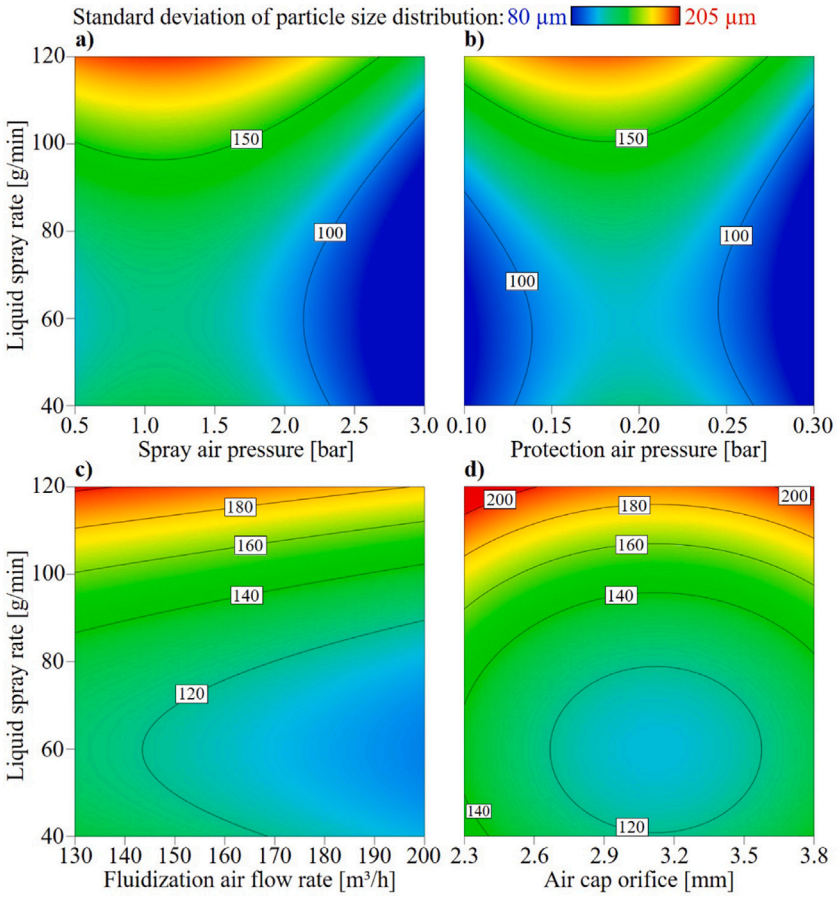

Fig. 11. Standard deviation of particle size distribution according to quadratic model at varied spray rate and (a) spray air pressure, (b) protection air pressure, (c) fluidization air flow rate, and (d) air cap orifice.

agglomerated particles stick to each other and form a connection. Due to this increased interaction of wet particles, agglomerates of many different sizes are built, which results in a wide particle size distribution with a high standard deviation. The wide spray zone created at increased spray rates further support this uneven growth, by providing a large zone for wet particles to form several liquid bridges and smaller drying zone. Since the binder solution was injected through two nozzles in bottom-spray configuration, the two spray cones might even interact with each other at high spray angles. Lastly, the standard deviation is increased due to breakage of larger agglomerates into smaller fragments, as the particle size distribution with a high mean agglomerate size is additionally widened when adding those small particles.

Fig. 11a and 11b show the influence of the spray air and protection air pressure on the standard deviation. With increasing pressures, the produced agglomerates have a narrower size distribution with smaller deviation. Due to the smaller spray cone angle at higher pressures, a narrow spray zone is created in front of both nozzles. This defined spray zone in combination with a larger drying zone limits the area in which wet particle collisions occur. Since the agglomerate size is generally smaller, particle fragments from broken agglomerates do not impact the width of the particle size distribution to the same extent as for a distribution with a higher mean diameter.

Analogously, the size distribution of the smaller agglomerates formed at high fluidization air volume flows is not as majorly affected by the fine particles generated in the process as the distribution of the larger agglomerates produced at low air flow. Furthermore, fine particles, such as spray dried droplets and dust generated by breakage and attrition, are more likely to be elutriated in a process with higher fluidization air flow. Since these elutriated particles are not part of the product, they do not influence the particle size distribution. Consequently, an increase in fluidization air flow results in a narrower size distribution and smaller standard deviation as shown in Fig. 11c.

Choosing an air cap with a larger orifice diameter leads to a higher spray air flow in order to achieve the same pressure compared to a smaller air cap (see Fig. 7). As can be seen in Fig. 11d and from Eq. (5), no general trend, that is applicable to the whole design space, could be observed. Due to the many significant interactions involving the air cap orifice, the standard deviation can be influenced either positively or negatively depending on the further parameter settings. One of these interactions is the combination of air cap orifice size and spray air pressure, which leads to a narrower size distribution with increasing value. Other relevant interactions include for example the interaction between the pressures of both nozzle air flows and the ALR, which is based on liquid spray rate and spray air pressure.

4. Conclusion

While spraying of the liquid is a crucial step in fluidized bed spray agglomeration, the correlation of the associated parameters, physicochemical phenomena occurring during the process, and agglomerate properties is yet to be fully explained. To contribute to a comprehensive understanding of the process, measurements of nozzle characteristics as well as agglomeration experiments were performed at varied spray parameters. For the agglomeration experiments, a statistical experimental plan including process variables as well as parameters regarding the nozzle set-up was created. Afterwards, the mean size and size distribution of the product particles was evaluated and the significant influences were combined in quadratic models.

Overall, the liquid spray rate, spray air and protection air pressure, and fludization air volume flow were identified as most influential factors on mean agglomerate size. For the standard deviation of the particle size distribution, the diameter of the air cap orifice is an additional main impact. Thereby, the spray rate mainly influences the amount of wet particles in the fluidized bed and the stability of liquid bridges formed between particles, which results in a high spray rate leading to larger agglomerates with a wider size distribution. Droplet size and velocity as well as spray cone angle were massively affected by the spray air, which subsequently influences the agglomeration in such a way that small particles with a narrow size distribution were formed at high pressure. A factor that has not been investigated before, the pressure of the protection air applied to the nozzle, showed a significant influence on spray pattern and agglomerate size, with an increasing pressure resulting in decreasing particle size and width of the distribution. Increasing the fluidization air flow lead to the production of smaller agglomerates with a narrow size distribution due to higher bed porosity and enhanced particle breakage. Lastly, several interactions between the various spray parameters further impact agglomerate formation.

By combining the data obtained from nozzle characterization and spray agglomeration experiments, this study correlates spray parameters, spray pattern and droplets characteristics, and agglomerate properties, which contributes to a better process understanding and provides a guideline to find suitable parameter setting to achieve desired product properties. In this way, a bridge is built between micro-mechanisms happening during agglomeration, as for example studied in [41,42], and macroscopic observations about process behavior and particle properties. The approach used in this study can easily be transferred to other material systems and fluidized bed set-ups and nozzles to obtain a better understanding about industrial processes and provide a foundation to optimize the agglomeration process as well as the product quality. By providing information on the influence of numerous parameters over a wide range and giving an overview of relevant factors and interactions, this study can serve as basis for future works with focus on other materials, fluidized bed set-ups, or the more detailed investigation of certain here mentioned effects.

Declaration of competing interest

The authors declare that they have no known competing financial interests or personal relationships that could have appeared to influence the work reported in this paper.

Data availability

Data will be made available on request.

Acknowledgments

This work was supported by Syntegon Technology.

Appendix A. Supplementary data

Supplementary material related to this article can be found online at https://doi.org/10.1016/j.powtec.2024.120274.

References

[1] H.G. Merkus, Particle size measurements: Fundamentals, practice, quality, particle Technology Series, vol. 17, Springer Netherlands, Dordrecht, 2009.
[2] D. Schulze, Pulver und Schüttgüter: Fließeigenschaften und Handhabung, fourth ed., VDI-Buch Chemische Technik/Verfahrenstechnik, Springer Vieweg, Berlin and Heidelberg, 2019.
[3] R. Boerefijn, M.J. Hounslow, Studies of fluid bed granulation in an industrial R&D context, Chem. Eng. Sci. 60 (14) (2005) 3879–3890, http://dx.doi.org/10.1016/j.ces.2005.02.021.
[4] G.K. Reynolds, J.S. Fu, Y.S. Cheong, M.J. Hounslow, A.D. Salman, Breakage in granulation: A review, Chem. Eng. Sci. 60 (14) (2005) 3969–3992, http://dx.doi.org/10.1016/j.ces.2005.02.029.
[5] B.J. Ennis, J.D. Litster, Particle size enlargement, in: D.W. Green, M.Z. Southard (Eds.), Perry's Chemical Engineers' Handbook, McGraw-Hill Education, New York, 2019, 20–56–20–89.
[6] H. Uhlemann, L. Mörl, Wirbelschicht-Sprühgranulation, VDI-Buch, Springer, Berlin and Heidelberg, 2000.
[7] S.M. Iveson, J.D. Litster, K. Hapgood, B.J. Ennis, Nucleation, growth and breakage phenomena in agitated wet granulation processes: a review, Powder Technol. 117 (1–2) (2001) 3–39, http://dx.doi.org/10.1016/S0032-5910(01)00313-8.
[8] P.D. Hede, P. Bach, A.D. Jensen, Two-fluid spray atomisation and pneumatic nozzles for fluid bed coating/agglomeration purposes: A review, Chem. Eng. Sci. 63 (14) (2008) 3821–3842, http://dx.doi.org/10.1016/j.ces.2008.04.014.
[9] B. Mulhem, G. Schulte, Effect of solid particle characteristics on suspension atomization, Atom. Sprays 13 (2–3) (2003) 23, http://dx.doi.org/10.1615/AtomizSpr.v13.i23.100.
[10] T. Richter, Zerstäuben von Flüssigkeiten: Düsen und Zerstäuber in Theorie und Praxis, fourth ed., utb-studi-e-book, vol. 5186, UTB GmbH and UVK, Stuttgart and Konstanz, 2017.
[11] L. Fries, Discrete Particle Modeling of a Fluidized Bed Granulator (Dissertation), Hamburg University of Technology, Hamburg, 2012.
[12] K.C. Link, E.-U. Schlünder, Fluidized bed spray granulation, Chem. Eng. Process.: Process Intensif. 36 (6) (1997) 443–457, http://dx.doi.org/10.1016/S0255-2701(97)00022-6.
[13] F. Ronsse, J.G. Pieters, K. Dewettinck, Modelling side-effect spray drying in top-spray fluidised bed coating processes, J. Food Eng. 86 (4) (2008) 529–541, http://dx.doi.org/10.1016/j.jfoodeng.2007.11.003.
[14] S. Karlsson, A. Rasmuson, B. van Wachem, I.N. Björn, CFD modeling of the Wurster bed coater, AIChE J. 55 (10) (2009) 2578–2590, http://dx.doi.org/10.1002/aic.11847.
[15] E.S.K. Tang, L. Wang, C.V. Liew, L.W. Chan, P.W.S. Heng, Drying efficiency and particle movement in coating–impact on particle agglomeration and yield, Int. J. Pharm. 350 (1–2) (2008) 172–180, http://dx.doi.org/10.1016/j.ijpharm.2007.08.047.
[16] M. Hemati, R. Cherif, K. Saleh, V. Pont, Fluidized bed coating and granulation: influence of process-related variables and physicochemical properties on the growth kinetics, Powder Technol. 130 (1–3) (2003) 18–34, http://dx.doi.org/10.1016/S0032-5910(02)00221-8.
[17] J. Bouffard, M. Kaster, H. Dumont, Influence of process variable and physicochemical properties on the granulation mechanism of mannitol in a fluid bed top spray granulator, Drug Dev. Ind. Pharmacy 31 (9) (2005) 923–933, http://dx.doi.org/10.1080/03639040500272124.
[18] U. Vengateson, R. Mohan, Experimental and modeling study of fluidized bed granulation: Effect of binder flow rate and fluidizing air velocity, Resour.-Efficient Technol. 2 (2016) S124–S135, http://dx.doi.org/10.1016/j.reffit.2016.10.003.
[19] M. Dadkhah, E. Tsotsas, Influence of process variables on internal particle structure in spray fluidized bed agglomeration, Powder Technol. 258 (2014) 165–173, http://dx.doi.org/10.1016/j.powtec.2014.03.005.
[20] D.M. Lipps, A.M. Sakr, Characterization of wet granulation process parameters using response surface methodology. 1. Top-spray fluidized bed, J. Pharmaceut. Sci. 83 (7) (1994) 937–947, http://dx.doi.org/10.1002/jps.2600830705.
[21] C. Wang, J. Ma, J. Cai, H. Pu, X. Chen, Influence of multi-factor interactions on particle growth during top-spray fluidized bed agglomeration, Particuology 94 (2024) 173–186, http://dx.doi.org/10.1016/j.partic.2024.08.003.
[22] I.C. Kemp, A. van Millingen, H. Khaled, Development and verification of a novel design space and improved scale-up procedure for fluid bed granulation using a mechanistic model, Powder Technol. 361 (2020) 1021–1037, http://dx.doi.org/10.1016/j.powtec.2019.10.093.
[23] G. Strenzke, R. Dürr, A. Bück, E. Tsotsas, Influence of operating parameters on process behavior and product quality in continuous spray fluidized bed agglomeration, Powder Technol. 375 (2020) 210–220, http://dx.doi.org/10.1016/j.powtec.2020.07.083.
[24] J. Du, A. Bück, E. Tsotsas, Influence of process variables on spray agglomeration process in a continuously operated horizontal fluidized bed, Powder Technol. 363 (2020) 195–206, http://dx.doi.org/10.1016/j.powtec.2020.01.008.
[25] V. Pont, K. Saleh, D. Steinmetz, M. Hémati, Influence of the physicochemical properties on the growth of solid particles by granulation in fluidized bed, Powder Technol. 120 (1–2) (2001) 97–104, http://dx.doi.org/10.1016/S0032-5910(01)00355-2.
[26] P. Rajniak, C. Mancinelli, R.T. Chern, F. Stepanek, L. Farber, B.T. Hill, Experimental study of wet granulation in fluidized bed: Impact of the binder properties on the granule morphology, Int. J. Pharm. 334 (1–2) (2007) 92–102, http://dx.doi.org/10.1016/j.ijpharm.2006.10.040.
[27] G.A. Hebbink, B.H. Dickhoff, Application of lactose in the pharmaceutical industry, in: M. Paques, C. Lindner (Eds.), Lactose, Elsevier, 2019, pp. 175–229, http://dx.doi.org/10.1016/B978-0-12-811720-0.00005-2.
[28] DFE Pharma, Lactochem® Fine Powder, 2023, https://dfepharma.com/excipients/lactochem-fine-powder/.

[29] K. Kramm, M. Orth, A. Teiwes, J.C. Kammerhofer, V. Meunier, S. Pietsch-Braune, S. Heinrich, Influence of nozzle parameters on spray pattern and droplet characteristics for a two–fluid nozzle, Chem. Ing. Tech. 95 (1–2) (2023) 151–159, http://dx.doi.org/10.1002/cite.202200152.
[30] AOM-Systems, SpraySpy® LabLine: Spray & droplet analysis for research & development, 2023, https://www.aom-systems.com/en/wp-content/uploads/2023/03/SpraySpy_LabLine_Product_info_2023.pdf.
[31] P.F. de Aguiar, B. Bourguignon, M.S. Khots, D.L. Massart, R. Phan-Than-Luu, D-optimal designs, Chemometr. Intell. Lab. Syst. 30 (2) (1995) 199–210, http://dx.doi.org/10.1016/0169-7439(94)00076-X.
[32] X. Liu, R. Xue, Y. Ruan, L. Chen, X. Zhang, Y. Hou, Effects of injection pressure difference on droplet size distribution and spray cone angle in spray cooling of liquid nitrogen, Cryogenics 83 (2017) 57–63, http://dx.doi.org/10.1016/j.cryogenics.2017.01.011.
[33] A.H. Lefebvre, Atomization and Sprays, Combustion, Taylor & Francis, Bristol, Pa., 1989.
[34] D. Newton, M. Fiorentino, G. Smith, The application of X-ray imaging to the developments of fluidized bed processes, Powder Technol. 120 (1–2) (2001) 70–75, http://dx.doi.org/10.1016/S0032-5910(01)00349-7.
[35] S. Ariyapadi, D.W. Holdsworth, C.J. Norley, F. Berruti, C. Briens, Digital X-ray imaging technique to study the horizontal injection of gas-liquid jets into fluidized beds, Int. J. Chem. React. Eng. 1 (1) (2003) http://dx.doi.org/10.2202/1542-6580.1114.
[36] N.K. Rizk, A.H. Lefebvre, Spray characteristics of plain-jet airblast atomizers, J. Eng. Gas Turbines Power 106 (3) (1984) 634–638, http://dx.doi.org/10.1115/1.3239617.
[37] C. Vesey, J. Cronlein, A. Breuer, S. Gerstner, Fluid bed nozzle spray characterization of an aqueous ethylcellulose dispersion for particle taste-masking applications, 2014, https://www.colorcon.com/component/flexicontent/download/312/553/34?method=view.
[38] P. Walzel, Liquid atomization, Int. Chem. Eng. (Q. J. Transl. Russia, Eastern Europe and Asia) 33 (1) (1993).
[39] B.J. Ennis, G. Tardos, R. Pfeffer, A microlevel-based characterization of granulation phenomena, Powder Technol. 65 (1–3) (1991) 257–272, http://dx.doi.org/10.1016/0032-5910(91)80189-P.
[40] D.N. Mazzone, G.I. Tardos, R. Pfeffer, The behavior of liquid bridges between two relatively moving particles, Powder Technol. 51 (1) (1987) 71–83, http://dx.doi.org/10.1016/0032-5910(87)80041-4.
[41] F. Bunke, S. Pietsch-Braune, S. Heinrich, Three-dimensional measurement method of binary particle collisions under dry and wet conditions, Chem. Eng. J. 489 (2024) 151016, http://dx.doi.org/10.1016/j.cej.2024.151016.
[42] P. Grohn, T. Oesau, S. Heinrich, S. Antonyuk, Investigation of the influence of impact velocity and liquid bridge volume on the maximum liquid bridge length, Adv. Powder Technol. 33 (6) (2022) 103630, http://dx.doi.org/10.1016/j.apt.2022.103630.
[43] M. Schmidt, A. Bück, E. Tsotsas, Shell porosity in spray fluidized bed coating with suspensions, Adv. Powder Technol. 28 (11) (2017) 2921–2928, http://dx.doi.org/10.1016/j.apt.2017.08.020.

Maike Orth is a doctoral student at the Institute of Solids Process Engineering and Particle Technology at the Hamburg University of Technology. There, she obtained a M.Sc. in Process Engineering with distinction in 2019. Her research interests include particle formulation in fluidized beds, particle characterization, and CFD-DEM simulations of fluidized bed processes.

Matthias Börner is heading the research and development department at a Syntegon site in Schopfheim, Germany. Syntegon is an equipment manufacturer of fluid bed and mixer technology for the pharmaceutical industry. Matthias Börner studied process engineering at the University of Magdeburg until 2008. After his studies he obtained a PhD-in 2013 about CFD-DEM simulations and experimental flow characterizations in fluid bed granulation equipment.

Swantje Pietsch-Braune is a senior engineer in the Institute of Solids Process Engineering and Particle Technology at Hamburg University of Technology. She obtained her PhD in 2018 on the experimental and numerical investigations of fluidization behavior and liquid injection in three-dimensional prismatic spouted beds. Her research is focused on particle formulation in fluidized beds and CFD-DEM simulations of these processes.

Stefan Heinrich obtained his diploma in Process Engineering and a doctoral degree at the University Magdeburg. After positions as Assistant and Junior Professor and a Habilitation, he became full professor at the TUHH and director of the Institute of Solids Process Engineering and Particle Technology in 2008. He is editor of Advanced Powder Technology and Particuology, chairman of the Working Party on Agglomeration and Bulk Solids Technology of VDI-ProcessNet and of the EFCE Working Party on Agglomeration. His main research interests are fluidized bed technology, mainly for drying and particle formulation, particle simulation methods as well as contact, deformation and breakage mechanics of particles. He received the DECHEMA-Prize 2015.